Q. J. R. Meteorol. Soc. (2001), **127**, pp. 1375–1388

Influence of the β-effect on non-modal baroclinic instability

By G. RIVIÈRE[1]*, B. L. HUA[2,1] and P. KLEIN[2,1]
[1]*Laboratoire de Météorologie Dynamique, France*
[2] *Laboratoire de Physique des Océans, France*

(Received 7 August 2000; revised 18 December 2000)

SUMMARY

We focus on the influence of the β-effect on the singular modes of baroclinic instability in the Phillips model. An analytical intercomparison between normal and singular modes for the Eady problem on an f-plane has already been performed, showing that the amplification rate of the singular mode for the kinetic-energy norm after a dimensional time of three days is about 1.2 times larger than for the normal mode. We show here that, in the presence of the β-effect, the maximum amplification rate of the singular mode can be 1.5 times larger than for the normal-mode case. This difference is due to the lesser stabilizing effect of β on the singular modes compared with the normal modes. This result is obtained for the case of equal layer depths which is relevant for the atmospheric situation. For the oceanic situation with unequal layer depths the amplification due to β is further increased leading to a factor of 1.8 in amplification rates between the two types of modes after a dimensional time of about 20 days. This behaviour is explained by the fact that β only intervenes in the anti-Hermitian part of the linear dynamical operator, the main effect of which is to alter the vertical phase tilt of the perturbations. As a consequence, the structure of the bi-orthogonal mode becomes more inclined to the vertical in the presence of β while, on the contrary, the structure of the unstable normal mode becomes less inclined.

KEYWORDS: Baroclinic instability β-effect Singular modes

1. INTRODUCTION

The behaviour of small disturbances under baroclinic instability is traditionally studied through the normal-modes approach, where the equations of motion are linearized about an appropriate background flow and are then solved for the eigenvectors of the linearized dynamical operator, Λ, which describes the evolution of the state vector, ϕ

$$\frac{\partial \phi}{\partial t} = \Lambda \phi. \tag{1}$$

If, initially, $\phi(0)$ is the eigenvector of Λ (i.e. it corresponds to the normal mode) with eigenvalue σ, then $\phi(t) = \phi(0)\, e^{\sigma t}$, and the time growth is exponential for any inner product. The flow stability is inferred from the behaviour versus spatial wave number of the real part of σ. Idealized models like those originally considered by Eady (1949) and Charney (1947) relied on the normal-modes method to explain cyclogenesis. Such an approach has been widely used to study cyclogenesis in mid latitudes because it gives the right order of magnitude for growth rates, phase speeds and spatial scales.

However, when compared with observations, the normal-modes approach failed to explain the initial rapid growth that accompanies explosive cyclogenesis. Specifically, Farrell (1982, 1984) showed that over the short time period typical of observed cyclogenesis, transient non-modal growth can dominate normal-mode growth, for the simple set-up of the Eady model. Furthermore, he argued that the transient evolution of the structures that occurs during observed cyclogenesis could not be explained by a single, fixed-form normal mode. His main idea consisted of finding the best initial state such that the solutions interacted constructively with the basic state. Rotunno and Fantini (1989) expressed the evolution of the perturbation solely in terms of the interactions between the two neutral normal modes of Eady's model for spatial wave numbers beyond the short-wave cut-off. Their results show that, because the neutral modes are not

* Corresponding author: Laboratoire de Météorologie Dynamique, ENS, 24 rue Lhomond, 75005 Paris, France.
e-mail: griviere@lmd.ens.fr

orthogonal for a given norm, they can interact to extract energy from the basic flow for finite time. On the other hand, Farrell (1989), O'Brien (1992) and Davies and Bishop (1994) addressed the more general problem of finding the optimal growth rate for a given physical inner product. Different methods were employed, among which were formulations based on a variational principle and/or identification of the bi-orthogonal of the most unstable normal mode. However, the most systematic derivation appeared with the introduction of singular modes. This method was introduced to meteorology by Lorenz (1965). It was further developed by Lacarra and Talagrand (1988) in order to study the initial evolution of error growth and to systematically determine the initial perturbation that optimizes the growth for a given inner product and for a specified finite time, T.

For a given inner product $\langle ., . \rangle_S$, the aim is to look for a perturbation that maximizes the amplification rate

$$\frac{\langle \phi(t), \phi(t) \rangle_S}{\langle \phi(0), \phi(0) \rangle_S}. \tag{2}$$

If we note, Φ the column vector formed by the canonical components of ϕ (the canonical basis being linked with a norm), and $\mathbf{A}$, the matrix of the dynamical operator Λ in this basis, it leads to the matrix equation

$$\frac{\partial \Phi}{\partial t} = \mathbf{A}\Phi, \tag{3}$$

and the associated resolvent $\mathbf{M}(t)$ is

$$\Phi(t) = \mathbf{M}(t)\Phi(0). \tag{4}$$

The amplification rate for the measure $\langle ., . \rangle_S$ is then

$$\frac{\langle \phi(t), \phi(t) \rangle_S}{\langle \phi(0), \phi(0) \rangle_S} = \frac{\Phi(t)^\star \mathbf{S} \Phi(t)}{\Phi(0)^\star \mathbf{S} \Phi(0)} = \frac{\Phi(0)^\star \mathbf{M}(t)^\star \mathbf{S}\mathbf{M}(t)\Phi(0)}{\Phi(0)^\star \mathbf{S}\Phi(0)}, \tag{5}$$

where $\mathbf{S}$ is the matrix representing the measure $\langle ., . \rangle_S$ and * indicates the conjugate transpose. The optimal solution is obtained when $\Phi(0)$ is the eigenvector of $\mathbf{S}^{-1}\mathbf{M}^\star(t)\mathbf{S}\mathbf{M}(t)$ which corresponds to the largest eigenvalue, the so-called singular mode. In most idealized models $\mathbf{A}$ does not depend on time, $\mathbf{M}(t) = \exp(\mathbf{A}t)$, and the singular eigenvalues are those of $\mathbf{S}^{-1} \exp(\mathbf{A}^\star t)\mathbf{S} \exp(\mathbf{A}t)$. This method was rapidly adopted for use in conjunction with the tangent-linear formulation of nonlinear models for the study of quite complex situations: Farrell and Moore (1992) and Moore and Farrell (1993) considered the case of quasi-geostrophic oceanic flows, while Borges and Hartmann (1992) and Yoden and Nomura (1993) dealt with a barotropic atmosphere. Joly (1995) studied the finite-time stability of steady atmospheric fronts. Juckes (1995) investigated the stability of shear lines on either the tropopause or the surface boundary. Singular modes are now used operationally for ensemble prediction in several weather-prediction centres in order to assess the spread, in the forecasts, consistent with the analysis errors.

Farrell and Ioannou (1996) elaborated in depth the usefulness of singular modes for the 'Generalized Stability Theory' of several types of flows, which can either be constant or variable in time. The same approach was also applied by Fischer (1998) to the Eady problem with uniform potential vorticity. It is found that the singular modes can depart significantly from the normal modes, though the dynamics of the problem are very simple. In contrast to the behaviour of normal modes, singular modes do not exhibit any short-wave cut-off. Moreover, for the short time limit, the optimal structure

for the kinetic-energy norm is such that there is a phase quadrature with height of the stream-function field, thus recovering a result found by Davies and Bishop (1994). For the long time limit (after approximately 3 days for the atmosphere), the wave number at which the most unstable singular mode is maximal (for the kinetic-energy norm) tends toward the optimal normal-mode wave number, but the optimal singular amplification rate still remains 20–25% larger than that of the optimal normal mode.

Hereafter, we have opted for the set-up of the Phillips (1954) model to carry out a systematic intercomparison between normal modes (NM hereafter) and singular modes (SM hereafter) for a given inner product (either kinetic-energy norm or potential-enstrophy norm) and for a specified finite time, T. Our main motivation for choosing this model is to provide an analytically tractable rationale for the influence of the β-effect which is discarded in Eady's formulation. In section 2, the linearized equations in the Phillips model are recalled. In section 3, analytical expressions for the short and long time limits are derived and the results of the differences in amplification rates and vertical structures between normal modes and singular modes are presented. Section 4 addresses the oceanic case where the two layer depths are unequal. A final discussion of our results is given section 5.

2. The Phillips model

The set-up is the two-layer quasi-geostrophic model on the β-plane of Phillips (1954) where U_j, H_j, ρ_j are, respectively, the constant zonal velocity of the basic state, depth and density of each layer $j = 1, 2$. Both the upper and lower surfaces are rigid. The linearized non-dimensional equations without friction are (see Pedlosky 1987):

$$\left(\frac{\partial}{\partial t} + U_j \frac{\partial}{\partial x}\right)\{\nabla^2 \phi_j - (-1)^j F_j(\phi_2 - \phi_1)\} + \{\beta - (-1)^j F_j(U_1 - U_2)\}\frac{\partial \phi_j}{\partial x} = 0, \tag{6}$$

$$F_j = \frac{f^2 L^2}{g\frac{\rho_2 - \rho_1}{\rho_0} H_j}, \quad \beta = \frac{L^2 \beta_{\mathrm{dim}}}{U}, \quad U_j = \frac{U_{j\mathrm{dim}}}{U}, \tag{7}$$

where ϕ_j is the stream-function perturbation in each layer, and the dim subscript denotes dimensional numbers. Without lack of generality, we will choose $U_1 = -U_2$, and the shear will be equal to $U_s = U_1 - U_2 = 2U_1$. In order to use the singular-vectors method we have to write the matrix equation associated with Eq. (6). The column state vector, $\Phi = A_1\mathbf{e}_1 + A_2\mathbf{e}_2$, is the stream function written in the orthonormal basis $(\mathbf{e}_1, \mathbf{e}_2)$ for the L_2 norm (applied to the stream function) with $\mathbf{e}_1 \propto (e^{ikx+ily}, 0)$, $\mathbf{e}_2 \propto (0, e^{ikx+ily})$ and k, l the horizontal wave numbers. Thus, the stream-function variance norm (proportional to the geopotential variance norm), for which $\mathbf{S}$ is the identity matrix, is $\Phi^*\Phi$. Then Eq. (6) can be written as:

$$\frac{\partial}{\partial t}\Phi = \mathbf{A}\Phi \tag{8}$$

with

$$\mathbf{A} = -\mathrm{i}B\begin{bmatrix} \kappa^4 - 2(\kappa^2 + a^{-1})\beta' + \kappa^2(a^{-1} - a) & -2(\kappa^2 + \beta') \\ 2(\kappa^2 - \beta') & -\kappa^4 - 2(\kappa^2 + a)\beta' + \kappa^2(a^{-1} - a) \end{bmatrix}. \tag{9}$$

We have introduced the following notations:

$$\kappa^2 \equiv \frac{k^2+l^2}{(F_1F_2)^{\frac{1}{2}}}, \quad k' \equiv \frac{k}{(F_1F_2)^{\frac{1}{4}}}, \quad \beta' \equiv \frac{\beta}{2U_1\sqrt{F_1F_2}},$$

$$a \equiv \sqrt{\frac{F_1}{F_2}} = \sqrt{\frac{H_2}{H_1}},$$

$$B \equiv \frac{U_1(F_1F_2)^{\frac{1}{4}}k'}{\kappa^2(\kappa^2+a+a^{-1})}.$$

Except for the oceanic case considered in section 4, we will choose hereafter $H_1 = H_2 = H$ (i.e. $a = 1$ and, therefore, $F_1 = F_2 = F$). Furthermore, without loss of generality, the velocity and length scales, U and L, are chosen such that $U_1 = (U_{1\mathrm{dim}})/U = 1$ and $F = 1$ (i.e. $L = R_\mathrm{d}$ with $R_\mathrm{d} \equiv \{\sqrt{gH(\rho_2-\rho_1)/\rho_0}\}/(f)$ the internal Rossby radius of deformation). This leads to the simplified expressions for $\mathbf{A}$ and B shown in appendix A. Classical normal-mode results for this matrix are recalled in appendix A. In what follows, σ_+ and σ_- are the eigenvalues of $\mathbf{A}$ and the associated eigenvectors are, respectively, the unstable normal mode Φ_+ and the stable normal mode Φ_-.

We consider dimensional values corresponding to the atmosphere similar to those of Fischer (1998): Coriolis parameter $f = 10^{-4}$ s^{-1}, half-height $H = 4500$ m, zonal wind $U_{1\mathrm{dim}} = 7.35$ m s^{-1}, Brunt–Väisälä frequency $N^2 = g(\rho_2-\rho_1)/(\rho_0 H) = 1.27 \times 10^{-4}$ s^{-2}. They yield $R_\mathrm{d} = 507$ km. Furthermore, using $\beta_\mathrm{dim} = 1.7 \times 10^{-11}$ m^{-1}s^{-1} leads to $\beta' = 0.297$. Then, the dimensional e-folding time corresponding to max(Re (σ_+)) is equal to 36 hours.

3. Comparison of the normal and singular modes

The kinetic-energy norm is proportional to the stream-function (or geopotential) variance norm since, from the linearized Eq. (6), the perturbation is monochromatic. Consequently, the singular modes for the two norms are equal and the associated amplification rates are the eigenvalues of $\mathbf{M}^\star\mathbf{M} = \exp(\mathbf{A}^\star t)\exp(\mathbf{A}t)$. If the dynamical operator $\mathbf{A}$ is Hermitian, then the normal modes are orthogonal and identical to the singular modes (indeed if $\mathbf{A} = \mathbf{A}^\star$, the eigenvectors of $\mathbf{M}^\star\mathbf{M} = \exp(2\mathbf{A}t)$ are those of $\mathbf{A}$). The difference between normal and singular modes is due to the anti-Hermitian part $\mathbf{A} - \mathbf{A}^\star$, the main effect of which is to alter the vertical phase tilt of the perturbation structures. An important point to emphasize is that the β-effect only comes into play in that anti-Hermitian part (see Eq. (9)), the other component in $\mathbf{A} - \mathbf{A}^\star$ being due to the vertical shear.

The normal-mode amplification rate is proportional to $\mathrm{e}^{2\mathrm{Re}(\sigma_+)t}$ where σ_+ is the largest eigenvalue of $\mathbf{A}$ (see appendix A) while the singular mode largest amplification rate is hereafter denoted $\lambda(t)$.

(a) *Short time limit*

This limit is obtained for $2\mathrm{Re}(\sigma_+)t \ll 1$ (e.g. $t = \mathcal{O}(6$ hours) in dimensional units) and leads to the simplification:

$$\mathbf{M}^\star\mathbf{M} = \exp(\mathbf{A}^\star t)\exp(\mathbf{A}t) \simeq \mathbf{I} + (\mathbf{A}^\star + \mathbf{A})t \tag{10}$$

$$\simeq \begin{bmatrix} 1 & 4\mathrm{i}B\kappa^2 t \\ -4\mathrm{i}B\kappa^2 t & 1 \end{bmatrix}. \tag{11}$$

For short times, the only part of **A** which intervenes comes from the Hermitian part $\mathbf{A} + \mathbf{A}^\star$, and β has thus no influence on the initial amplification rate. This result is quite general and can be easily shown to remain valid for all types of norms (in particular for the kinetic-energy and enstrophy norms). The singular modes which are optimal for short times are, therefore, independent of β. The vertical structure of these singular modes is characterized by a phase lag of $\pi/2$ between ϕ_1 and ϕ_2, with $|\phi_1| = |\phi_2|$. Indeed, the maximum eigenvalue of $\mathbf{M}^\star\mathbf{M}$ is $1 + 4B\kappa^2 t$ and its associated eigenvector is $(1, -\mathrm{i})$. This result has already been noted by Davies and Bishop (1994) and Warrenfeltz and Elsberry (1989). This property is due to the fact that all the coefficients of **A** are pure imaginary.

(*b*) *Long time limit*

For the long time limit, i.e. for $\mathrm{e}^{2\mathrm{Re}(\sigma_+)t} \gg 1$ (which corresponds to t equal to or larger than $\mathcal{O}$(48 hours) in dimensional units), we can restrict ourselves to the unstable band of wave numbers of normal-mode theory ($\kappa_{1c} < \kappa < \kappa_{2c}$, with κ_{1c} and κ_{2c} the two wave-number cut-offs (see appendix A)). Indeed it can be shown that the wave number with the maximum amplification for the kinetic-energy norm lies inside this band for $\mathrm{e}^{2\mathrm{Re}(\sigma_+)t} \gg 1$. For this long time limit, it is possible to find an analytical relation between $\mathrm{e}^{2\mathrm{Re}(\sigma_+)t}$ and $\lambda(t)$ (see appendix B):

$$\lambda = \frac{\mathrm{e}^{2\mathrm{Re}(\sigma_+ t)}}{|a_- - a_+|^2}(1 + |a_+|^2)(1 + |a_-|^2) \equiv \alpha\, \mathrm{e}^{2\mathrm{Re}(\sigma_+ t)}, \tag{12}$$

where $a_\pm$ are related to the components of the eigenvectors of **A** (see appendix A). For a given wave number, the ratio α of the amplifications of the SM to the NM only depends on parameters of the system. Using the expression for $a_\pm$ (given by Eq. (A.4)), we obtain:

$$\alpha \equiv \frac{\lambda}{\mathrm{e}^{2\mathrm{Re}(\sigma_+ t)}} \equiv \frac{\kappa^4}{\kappa^4 - \frac{\kappa^8}{4} - \beta'^2}. \tag{13}$$

For $\kappa = 1$ and with $\beta' = 0.297$ we obtain $\alpha = 1.51$, while with $\beta' = 0$, $\alpha = 1.33$, showing that β has a quantitatively significant influence on the SM.

Let us now examine the vertical structure of the different modes. The eigenvector associated with λ when $\mathrm{e}^{2\mathrm{Re}(\sigma_+)t} \gg 1$, is the vector Φ_∞ defined in appendix B. This vector is orthogonal to the stable normal mode Φ_- and is, therefore, the bi-orthogonal to the unstable normal mode Φ_+ (see appendix B, Eq. (B.5)). This is a well known result of 'Generalized Stability Theory' (see Farrell and Ioannou 1996) that, when the normal modes are not orthogonal, the perturbation for optimal growth in the long time limit is not the unstable normal mode but its bi-orthogonal. If $a_+ = r\, \mathrm{e}^{-\mathrm{i}\theta}$, the most unstable NM, Φ_+, presents a vertical westward tilt which is characterized by a phase lag, θ, between ϕ_1 and ϕ_2, while the bi-orthogonal Φ_∞ has a phase lag equal to $\pi - \theta$. The main effect of β is concomitantly to decrease the value of θ (see appendix A) and, therefore, to increase the value of the phase lag of the bi-orthogonal, $\pi - \theta$. The efficiency of the bi-orthogonal is linked to its phase lag which increases with β. Thus, in the presence of β, the westward tilt of Φ_+ becomes less inclined to the vertical whereas the opposite is true for Φ_∞. Thus, β will exaggerate the differences between the normal-mode structure and its bi-orthogonal.

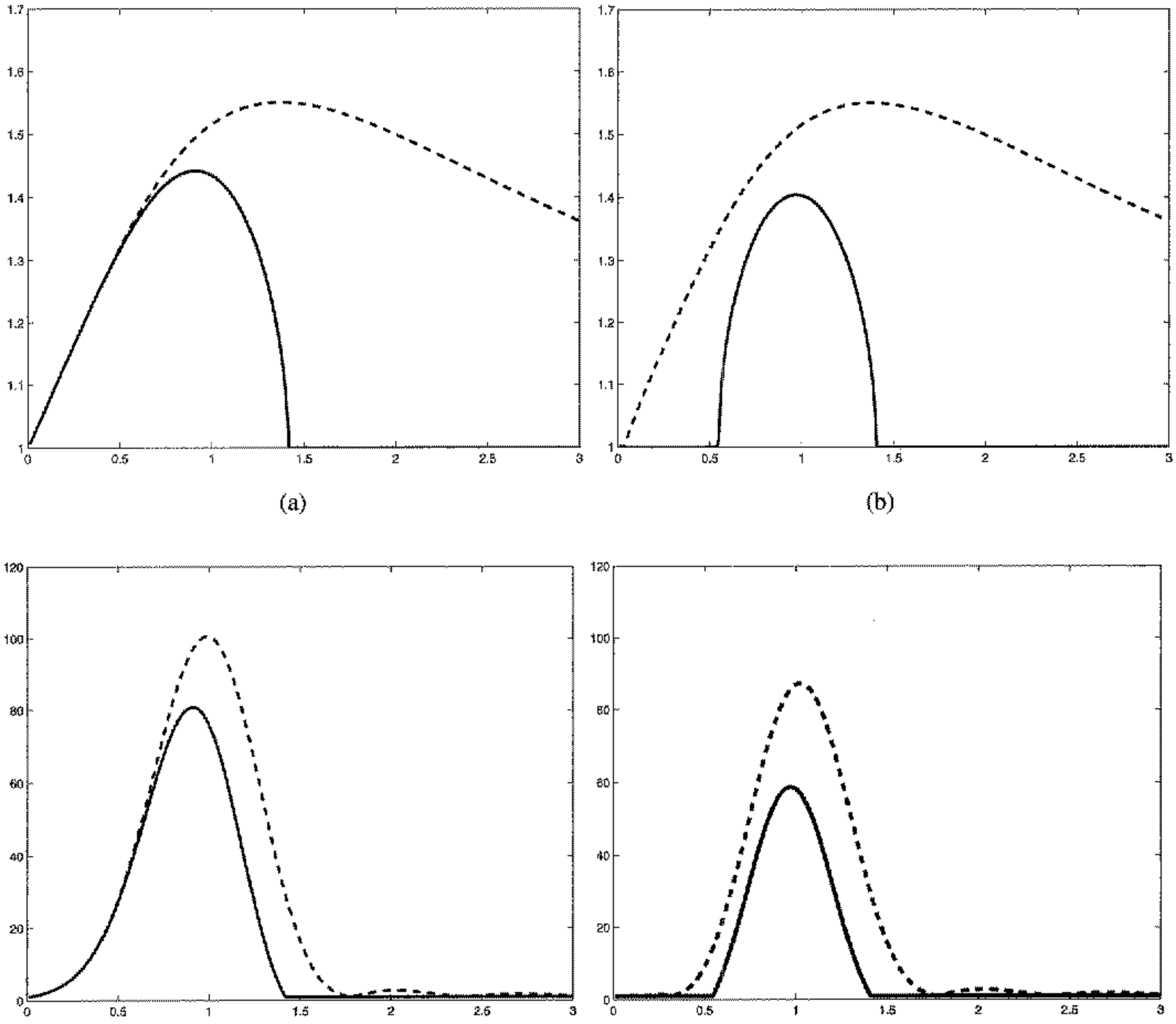

Figure 1. Amplification rates for the kinetic-energy norm versus horizontal wave number, in units of 2×10^{-6} m^{-1}. Normal mode, $\exp\{2\mathrm{Re}(\sigma_+)t\}$ (continuous line); singular mode, $\lambda(t)$ (dashed line). (a) $t = 6$ hours, $\beta = 0$, (b) $t = 6$ hours, $\beta = 1.7 \times 10^{-11}$ m^{-1}s^{-1}, (c) $t = 72$ hours, $\beta = 0$, (d) $t = 72$ hours, $\beta = 1.7 \times 10^{-11}$ m^{-1}s^{-1}. See text for further details.

(*c*) *Amplifications*

Let us first consider the results in the absence of β for the kinetic-energy norm. Amplification rates of NMs and SMs (respectively, $e^{2\mathrm{Re}(\sigma_+)t}$ and $\lambda(t)$) versus horizontal wave number are compared for two different optimization times: the short time limit (Fig. 1(a)) corresponding to $t = 6$ hours in dimensional units, and the long time limit (Fig. 1(c)) corresponding to $t = 72$ hours. λ reaches a maximum at a finite wave number larger than that corresponding to the radius of deformation. It has no short-wave cut-off and tends to 1 for high wave numbers. At small wave numbers the SM curve is close to the NM curve for all optimization times. Near the cut-off wave number for short times (Fig. 1(a)), the SM is largely amplified, and it is in the vicinity of this wave number that the difference between the SM and NM is the largest. For $\kappa > \kappa_{2c}$, interactions between two neutral non-orthogonal waves can be constructive as shown by Rotunno and Fantini (1989). For such wave numbers, no structure can remain stationary and the behaviour for any perturbation is sinusoidal in time (see appendix B). After a long time (Fig. 1(c)), the wave number with maximum λ tends to that of NM, but λ is still 25% larger than NM.

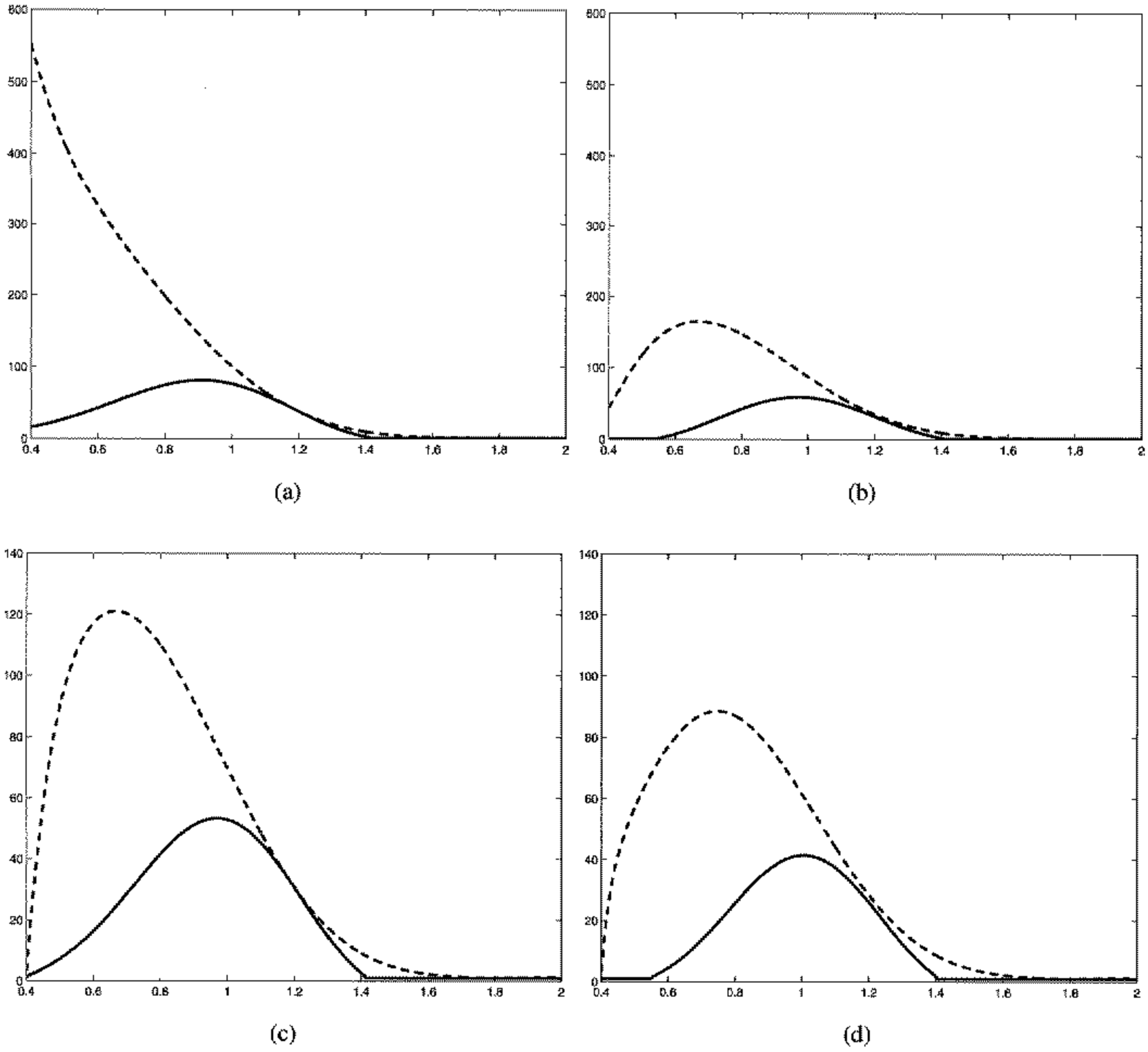

Figure 2. Amplification rates for the potential-enstrophy norm versus horizontal wave number, in units of 2×10^{-6} m^{-1}. Normal mode, $\exp\{2\mathrm{Re}(\sigma_+)t\}$ (continuous line); singular mode, $\lambda_{\mathrm{Ens}}(t)$ (dashed line). (a) $t =$ 72 hours, $\beta = 0$, $l = 0$, (b) $t = 72$ hours, $\beta = 1.7 \times 10^{-11}$ m^{-1}s^{-1}, $l = 0$, (c) $t = 72$ hours, $\beta = 0$, $l = 0.4/R_{\mathrm{d}}$, (d) $t = 72$ hours, $\beta = 1.7 \times 10^{-11}$ m^{-1}s^{-1}, $l = 0.4/R_{\mathrm{d}}$. See text for further details.

The above results corroborate the main results of Fischer (1998) for the Eady problem without β.

Let us now consider the influence of the β-effect on the NM and SM, still for the case of the kinetic-energy norm. Figures 1(b) and (d) correspond to the same specified finite times as Figs. 1(a) and (c), respectively. After a short time (Fig. 1(b)), we remark that λ is unchanged, proving that β does not influence the growth for short times as already anticipated analytically. We have found that the sensitivity to the β-effect only occurs after a larger time ($t > 24$ hours in dimensional units). At small wave numbers, because of the existence of a wave-number cut-off, $\kappa_{1\mathrm{c}}$, in the NM in the presence of β, the two types of modes behave very differently. For the long time limit (Fig. 1(d)), the unstable band of wave numbers for the SM is approximately equivalent to the unstable normal band. More precisely, the wave number which maximizes λ tends to that of the maximum NM. However, the major difference is that the maximum SM is now 50% larger than the maximum NM, while that value only reached 25% for $\beta = 0$. This larger difference in amplification rates is due to the fact that β has a lesser stabilizing influence

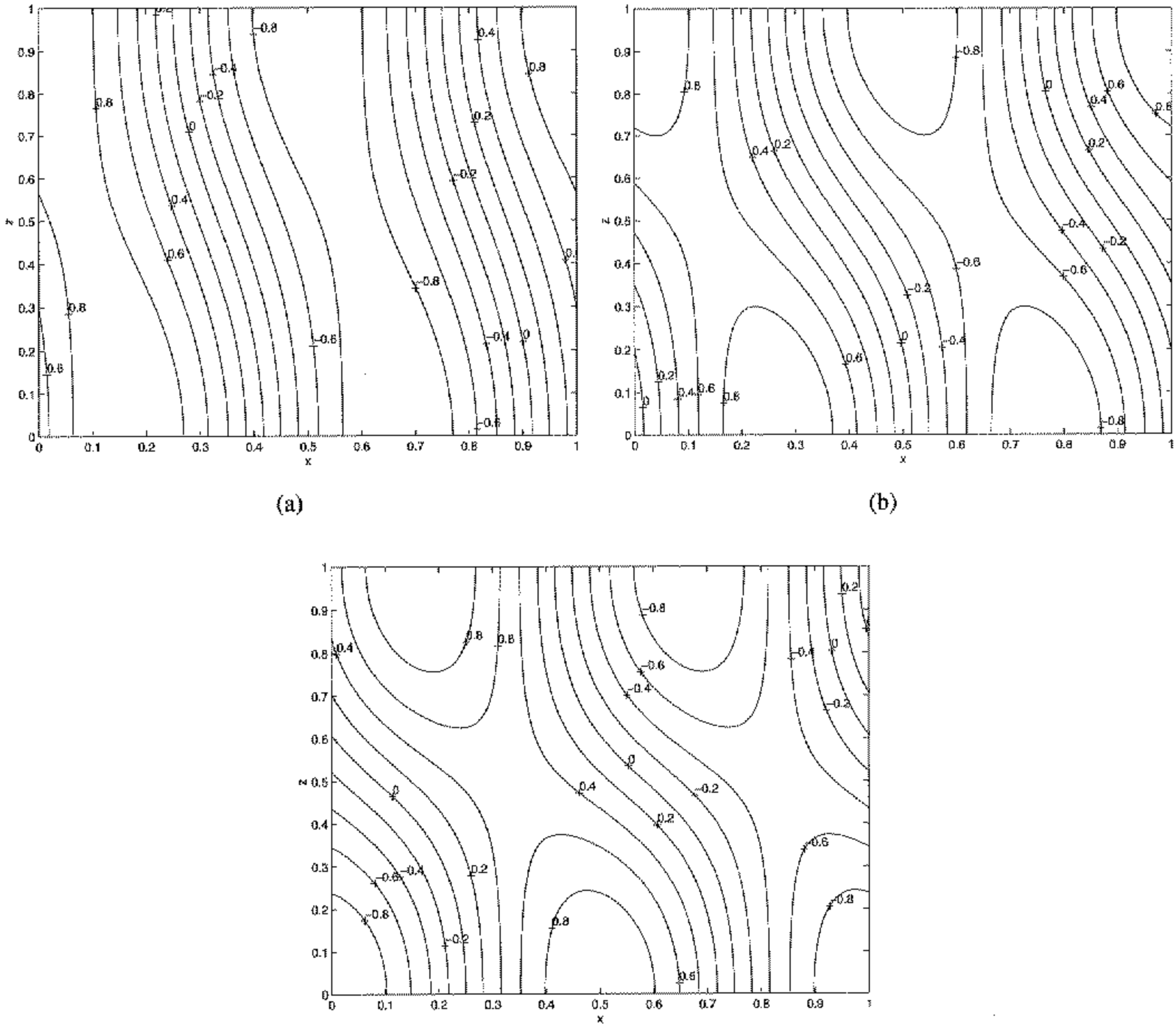

Figure 3. Vertical structure of the stream-function field for $\kappa = 1$. (a) Normal mode, (b) singular mode for the kinetic-energy norm optimized for $t = 6$ hours, (c) bi-orthogonal for the kinetic-energy norm. See text for further details.

on the SM than on the NM, as already shown in section 3(b). When taking into account Ekman friction (not shown here), we have found that the differences between the SM and NM are not modified quantitatively leading to the conclusion that friction has no influence on the intercomparison SM–NM.

The case of the potential-enstrophy norm was also studied by intercomparing the maximum amplification ($\lambda_{\mathrm{Ens}}(t)$) of the SM with the NM amplification $\mathrm{e}^{2\mathrm{Re}(\sigma_+)t}$. From the discussion of the introduction, $\lambda_{\mathrm{Ens}}(t)$ is the largest eigenvalue of the matrix $\mathbf{S}^{-1}\mathbf{M}^{\star}(t)\mathbf{S}\mathbf{M}(t)$ with

$$\mathbf{S} = \begin{pmatrix} -(\kappa^2+1) & 1 \\ 1 & -(\kappa^2+1) \end{pmatrix}^2. \tag{14}$$

In the case $l = 0$ and $\beta = 0$ (Fig. 2(a)) $\lambda_{\mathrm{Ens}}(t)$ becomes infinite for short wave numbers. With $\beta \neq 0$, $l = 0$ (Fig. 2(b)), $\beta = 0$, $l \neq 0$ (Fig. 2(c)) or $\beta \neq 0$, $l \neq 0$ (Fig. 2(d)), the $\lambda_{\mathrm{Ens}}(t)$ curve is bell shaped and reaches a maximum at a finite wave number smaller than the radius of deformation. For the long time limit, this wave number will tend to that of the maximum NM but less rapidly than for the kinetic-energy norm. In contrast

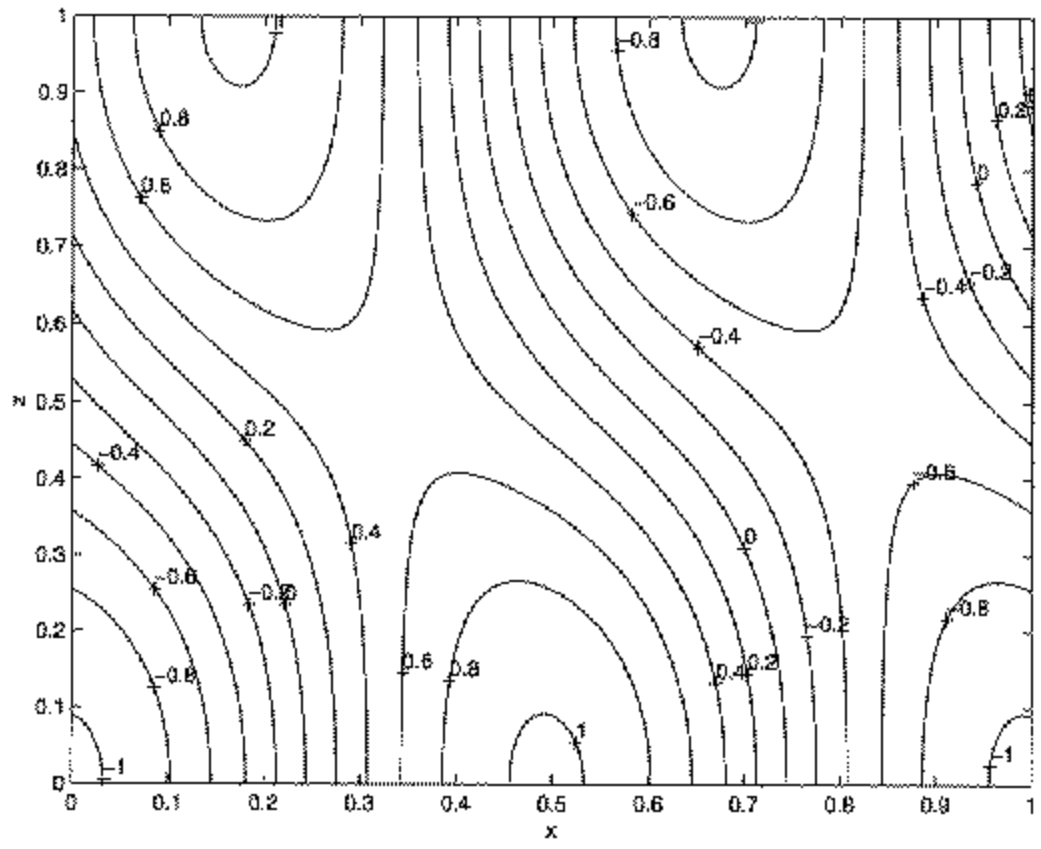

(a)

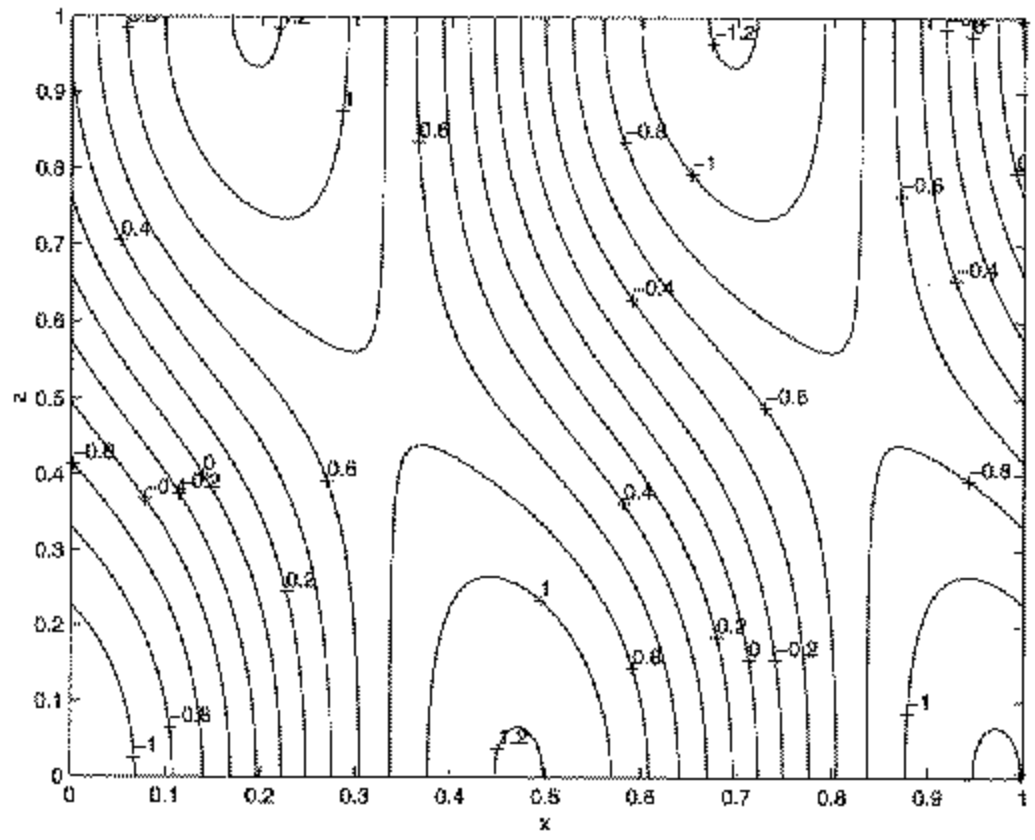

(b)

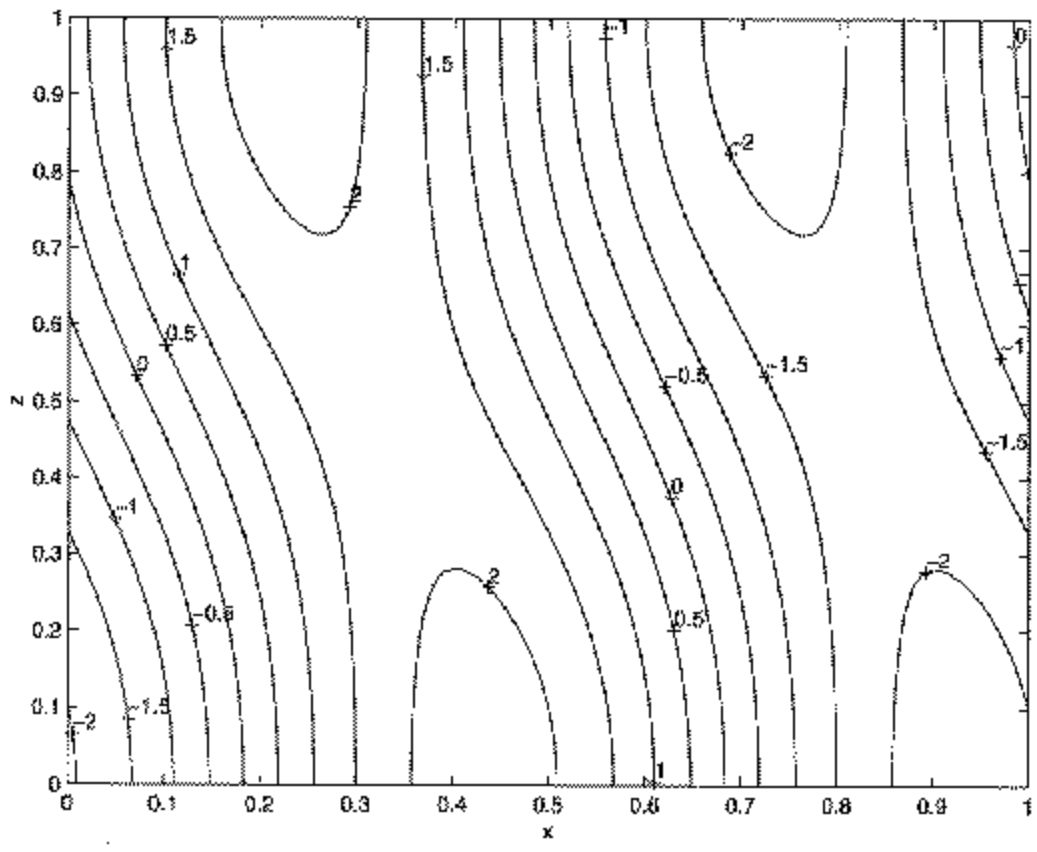

(c)

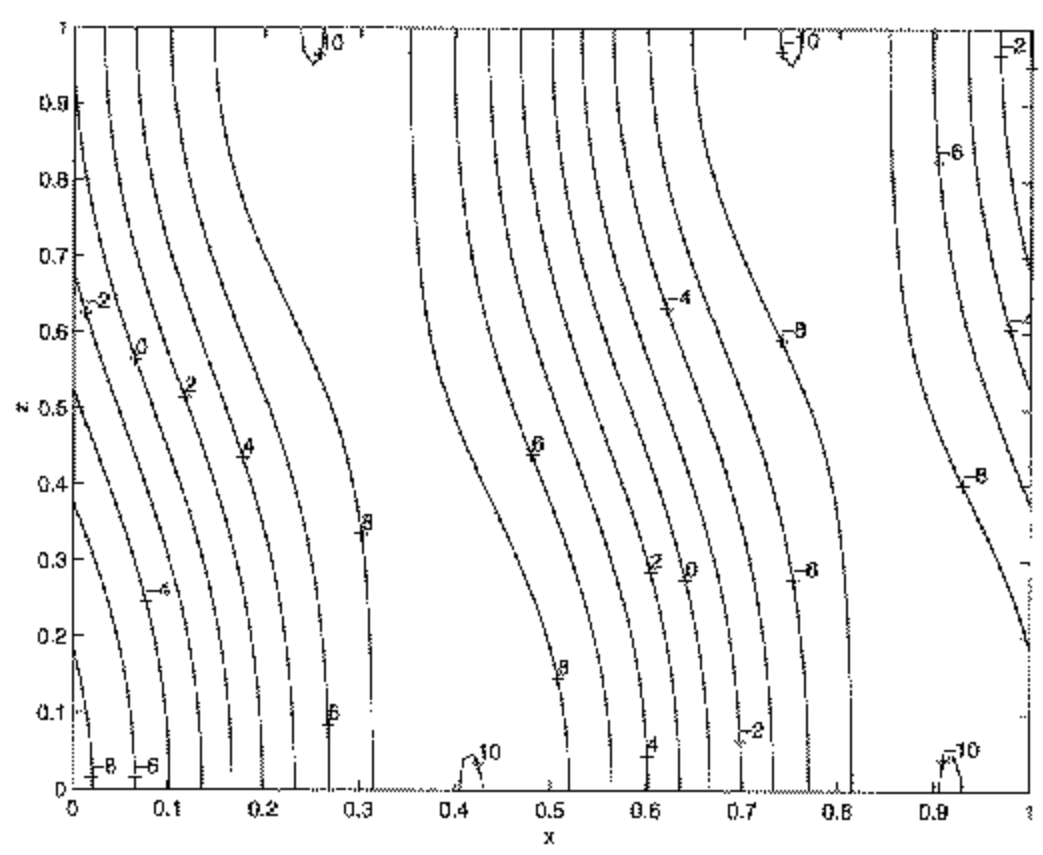

(d)

Figure 4. Time evolution of the vertical structure of the stream-function field for an initial perturbation corresponding to the bi-orthogonal for the kinetic-energy norm: $\Phi(0) \equiv \Phi_\infty$, for $\kappa = 1$. (a) Φ (1 hour), (b) Φ (6 hours), (c) Φ (24 hours), (d) Φ (72 hours). See text for further explanation.

to the kinetic-energy norm for the long time limit, the wave number with the maximum λ_{Ens} in Figs. 2(b)–(d) does not correspond to the wave number of the maximum NM: the unstable band for the potential-enstrophy norm is not yet close to the unstable normal band, because of the persistence of the instability of the small wave numbers ($\kappa < \kappa_{1c}$). The main difference between the kinetic-energy and potential-enstrophy norms is due to the role of the smallest wave numbers ($k \to 0$) where the contribution of the potential part (which is proportional to the temperature variance) dominates: the limit $k \to 0$ is also discussed in Juckes (1995).

If we restrict our study of the β-effect to the unstable normal band, for $\mathrm{e}^{2\mathrm{Re}(\sigma_+)t} \gg 1$, one can easily find analytically the relation between λ, λ_{Ens} and $\mathrm{e}^{2\mathrm{Re}(\sigma_+)t}$:

$$\lambda_{\mathrm{Ens}} = \frac{\mathrm{e}^{2\mathrm{Re}(\sigma_+ t)}}{\kappa^4 - \frac{\kappa^8}{4} - \beta'^2} \equiv \frac{\lambda}{\kappa^4}. \tag{15}$$

We remark that for $\kappa = 1$, the two amplifications λ and λ_{Ens} are equal. Furthermore, for a given wave number for $\mathrm{e}^{2\mathrm{Re}(\sigma_+)t} \gg 1$, $\lambda_{\mathrm{Ens}} = \lambda/\kappa^4$ and the factor of proportionality

between λ_{Ens} and λ does not depend on β. Inside the unstable normal band for a given wave number the β-effect is the same for the two norms.

(*d*) *Vertical structures*

We shall only consider here wave numbers located in the unstable normal band. It is well known that the NM has a stationary spatial structure and that any perturbation tends to this structure for long times. Indeed, in the limit $e^{2\mathrm{Re}(\sigma_+)t} \gg 1$, for any $\Phi(0)$, $\Phi(t) = \mathbf{M}(t)\Phi(0)$ is proportional to Φ_+ (see appendix B). However, the NM does not have the optimal structure (i.e. a phase quadrature) to extract energy from the basic flow most efficiently (the NM vertical structure has a phase lag $\theta < \pi/2$, Fig. 3(a))*. This is why the SM differs from the NM. But SM structures which differ from NM structures are non-stationary because of two effects included in the anti-Hermitian part of **A**: firstly the vertical shear and secondly the β-effect. This is why the quadrature is only the optimal structure for short times. For longer times, Warrenfeltz and Elsberry (1989) for the Phillips model, and Davies and Bishop (1994) for the Eady model, noticed that the optimal structure has a slope more inclined to the vertical than the quadrature and this is also clearly seen in the vertical structures of the SM of Fischer (1998). Finally, the initial phase lag of any SM lies between $\pi/2$ (optimization for short times, Fig. 3(b)) and $\pi - \theta$ (optimization for long times corresponding to the bi-orthogonal, Fig. 3(c)). If $\Phi(0) = \Phi_\infty$ (i.e. a system which is initialized with the bi-orthogonal), we see in Figs. 4(a)–(d) that the evolution of the perturbation towards the normal structure is very rapid, particularly so within the short time limit: this is due to the rotation effect of the anti-Hermitian part of **A**. After one day, the vertical structures $\Phi(t)$ and Φ_+ are already quite similar.

4. The oceanic case

In contrast to the large-scale tropospheric stratification which can be approximated by a constant Brunt–Väisälä profile, the oceanic mid-latitude stratification presents a pronounced peak in its Brunt–Väisälä profile in the vicinity of the main thermocline. This feature can be captured in a two-layer model by choosing quite different values for the depths of the layers: in the case of the Phillips model, this leads to the well known assymmetry between eastward and westward shears when the β-effect is taken into account (Pedlosky 1987).

For different layer depths ($H_1 \neq H_2$), it is also possible to find a relation between the SM and NM in the presence of the β-effect:

$$\lambda = \frac{\kappa^4}{\kappa^4 - \frac{\kappa^8}{4} - \beta'^2 - \frac{(a-a^{-1})}{2}\beta'\left(\kappa^4 + \frac{(a-a^{-1})}{2}\beta'\right)} e^{2\mathrm{Re}(\sigma_+ t)}. \tag{16}$$

This last equation shows that, for $\beta = 0$, there is no difference between equal and unequal layer depths. However, for $\beta \neq 0$, using a typical oceanic value of $H_1 = H_2/4$ (which leads to $a = 2$), we find that, for $\kappa = 1$, α reaches 1.8, whereas without β its value is 1.33. The influence of β on the intercomparison SM–NM is, therefore, further accentuated in the oceanic case. Figures 5(a) and (b) are equivalent to Figs. 1(c) and (d) but for the oceanic case. They show that for the long time limit, i.e. $t = 24$ days (corresponding to the oceanic parameter settings), the SM is 1.8 times larger than the NM.

* The vertical structure of the two-layer stream function, $\Phi = A_1\mathbf{e}_1 + A_2\mathbf{e}_2$ is defined in Figs. 3 and 4 by $\Phi(x, z) = \mathrm{Re}([\{(A_1 + A_2)/2\} - \{(A_1 - A_2)/2\}\cos(\pi z)]\exp\{2i\pi x\})$ for $z \in [0, 1]$ and $x \in [0, 1]$.

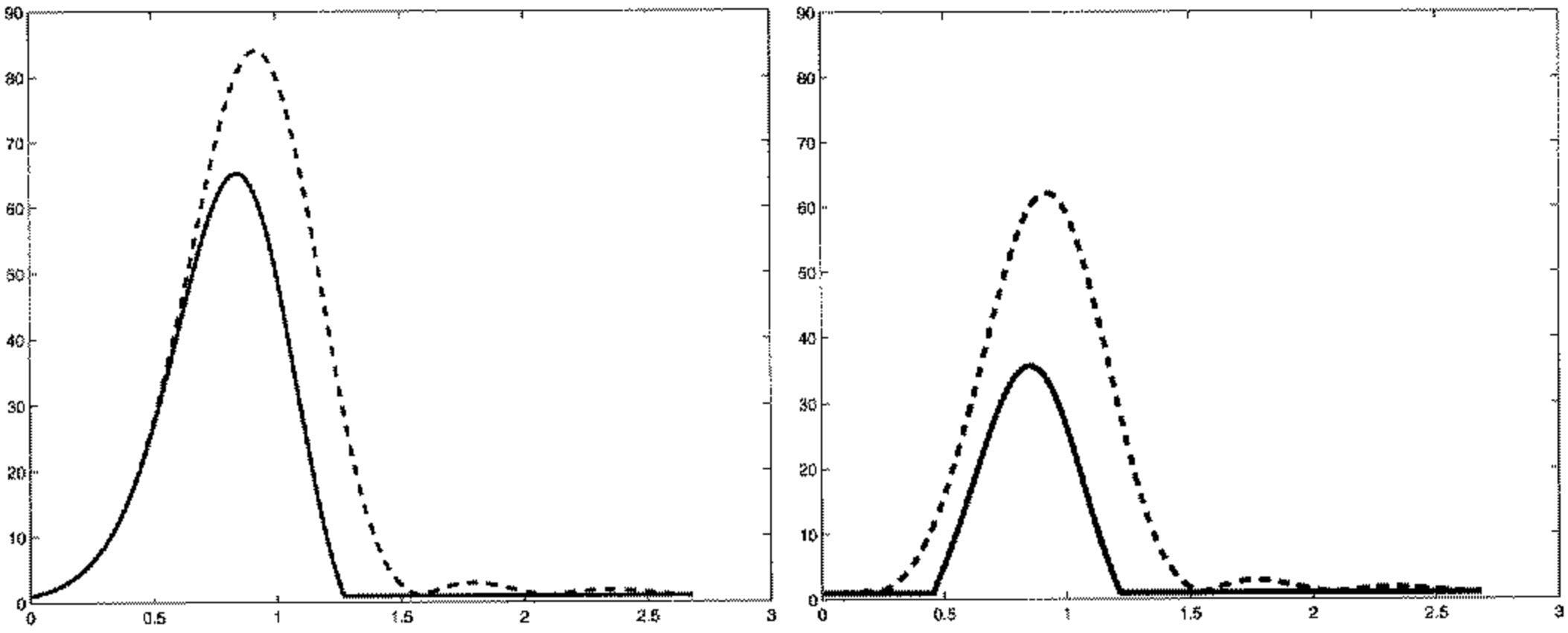

(a) (b)

Figure 5. Amplification rates for the kinetic-energy norm in the oceanic case where $H_1 = H_2/4$ versus horizontal wave number, in units of 18×10^{-6} m^{-1}. Normal mode, $\exp\{2\mathrm{Re}(\sigma_+)t\}$ (continuous line); singular mode, $\lambda_{\mathrm{Ens}}(t)$ (dashed line). (a) $t = 24$ days, $\beta = 0$, (b) $t = 24$ days, $\beta = 1.7 \times 10^{-11}$ m^{-1}s^{-1}. See text for further details.

5. Conclusion

A systematic analytical study of the β-effect on singular modes for finite time has been carried out for both the kinetic-energy and the potential-enstrophy norms. β solely intervenes in the anti-Hermitian part of $\mathbf{A}$ which is the crucial term for the differences in behaviour between the normal and singular modes. This part plays a significant role only after a finite time (for atmospheric parameter settings, the β-effect starts to have a quantitative influence for $t > 24$ hours). This anti-Hermitian part affects the vertical phase tilt of the perturbation structures and it is well known that the energy exchange between the basic flow and perturbations is strongly sensitive to this vertical structure. β is the only parameter that is completely included in the anti-Hermitian part. This rationalizes the effect of β on the singular modes and explains why the amplification rate for these modes is 1.5 times larger than for the normal modes. For a geometry with different layer depths, the effect of β on the vertical phase tilt is accentuated and the singular modes' amplification rate is 1.8 times larger than that of the normal modes after 24 days (which corresponds to the long time limit in the oceanic case).

Furthermore, we showed that in the normal unstable band, for a given wave number, the β-effect is the same for the kinetic-energy and the potential-enstrophy norms: it has a lesser stabilizing influence on the singular modes than on the normal modes. For the potential-enstrophy norm singular modes have a maximum for $\beta \neq 0$ or $l \neq 0$. The wave number corresponding to this maximum is smaller than the radius of deformation. The particularity of singular modes for this norm is that after 3 days (for the atmospheric parameter settings) the most unstable band is not the normal unstable band: small wave numbers below the wave-number cut-off are still very unstable.

Appendix A

Normal modes of the Phillips model

Without friction and with equal layer depths, the linearized operator is:

$$\mathbf{A} \equiv -\mathrm{i}B \begin{bmatrix} \kappa^4 - 2(\kappa^2 + 1)\beta' & -2(\kappa^2 + \beta') \\ 2(\kappa^2 - \beta') & -\kappa^4 - 2(\kappa^2 + 1)\beta' \end{bmatrix} \tag{A.1}$$

with $B = k'/\{\kappa^2(\kappa^2+2)\}$.

The eigenvalues of **A** are:

$$\sigma_\pm = B\{2\mathrm{i}(\kappa^2+1)\beta' \pm \sqrt{-\kappa^8+4\kappa^4-4\beta'^2}\}, \tag{A.2}$$

with eigenvectors

$$\Phi_\pm = \begin{pmatrix} 1 \\ a_\pm \end{pmatrix}, \tag{A.3}$$

such as

$$a_\pm = \frac{\kappa^4 - \pm\mathrm{i}\sqrt{-\kappa^8+4\kappa^4-4\beta'^2}}{2(\kappa^2+\beta')}. \tag{A.4}$$

There are two wave-number cut-offs, $\kappa = \kappa_{1c}$ and $\kappa = \kappa_{2c}$, which satisfy the equation

$$-\kappa^8 + 4\kappa^4 - 4\beta'^2 = 0. \tag{A.5}$$

If we note $a_+ = r\,\mathrm{e}^{-\mathrm{i}\theta}$, then the unstable normal mode Φ_+ has a phase lag θ between ϕ_1 and ϕ_2 (the stream-function perturbation in layers 1 and 2) such that

$$\tan(\theta) = \frac{\sqrt{-\kappa^8+4\kappa^4-4\beta'^2}}{\kappa^4}. \tag{A.6}$$

As θ decreases with β, the vertical normal-mode structure is less inclined to the vertical. If we initialize the system with the unstable normal mode $\Phi(0) = \Phi_+$, the amplification rate for all norms is (using Eqs. (3), (4) and (5)):

$$\frac{\langle\phi(t),\phi(t)\rangle}{\langle\phi(0),\phi(0)\rangle} = \exp\{2\mathrm{Re}(\sigma_+)t\}. \tag{A.7}$$

Appendix B

Singular modes of the Phillips model

In general, the resolvent $\mathbf{M} = \exp(\mathbf{A}t)$ can be obtained from the eigenvectors and eigenvalues of **A**. We have:

$$\mathbf{A} = \mathbf{P}\begin{bmatrix}\sigma_+ & 0\\ 0 & \sigma_-\end{bmatrix}\mathbf{P}^{-1}, \quad \text{with } \mathbf{P} = \begin{bmatrix}1 & 1\\ a_+ & a_-\end{bmatrix}, \tag{B.1}$$

which leads to:

$$\mathbf{M} = \mathbf{P}\begin{bmatrix}\mathrm{e}^{\sigma_+ t} & 0\\ 0 & \mathrm{e}^{\sigma_- t}\end{bmatrix}\mathbf{P}^{-1} = \frac{-1}{a_+-a_-}\begin{bmatrix}a_-\,\mathrm{e}^{\sigma_+ t} - a_+\,\mathrm{e}^{\sigma_- t} & -\mathrm{e}^{\sigma_+ t} + \mathrm{e}^{\sigma_- t}\\ a_+a_-(\mathrm{e}^{\sigma_+ t} - \mathrm{e}^{\sigma_- t}) & -a_+\,\mathrm{e}^{\sigma_+ t} + a_-\,\mathrm{e}^{\sigma_- t}\end{bmatrix}, \tag{B.2}$$

and the eigenvalues of $\mathbf{M}^\star\mathbf{M}$ are easily computed* (see appendix in Fischer (1998)).

In the long time limit, for the unstable normal band ($\mathrm{e}^{2\mathrm{Re}(\sigma_+)t} \gg 1$), **M** and, therefore, $\mathbf{M}^\star\mathbf{M}$ can be simplified:

$$\mathbf{M}^\star\mathbf{M} \simeq \frac{\mathrm{e}^{2\mathrm{Re}(\sigma_+)t}}{|a_- - a_+|^2}(1+|a_+|^2)\begin{bmatrix}|a_-|^2 & -a_+\\ -a_- & 1\end{bmatrix}. \tag{B.3}$$

* For the sake of simplicity, the analysis is restricted to the norms for which $\mathbf{S} = \gamma\mathbf{I}$ with **I** the identity matrix and γ a scalar.

The largest eigenvalue, λ, of $\mathbf{M}^*\mathbf{M}$ is:

$$\lambda = \frac{e^{2\mathrm{Re}(\sigma_+ t)}}{|a_- - a_+|^2}(1 + |a_+|^2)(1 + |a_-|^2), \tag{B.4}$$

and its associated eigenvector is the bi-orthogonal of Φ_+:

$$\Phi_\infty = \begin{pmatrix} a_+ \\ -1 \end{pmatrix}. \tag{B.5}$$

In the stable normal bands ($\kappa < \kappa_{1c}$ or $\kappa > \kappa_{2c}$), the two neutral normal modes in these bands are not orthogonal and can, therefore, interact to extract energy from the basic flow (Held 1985; Rotunno and Fantini 1989). Each perturbation can be expressed as a linear combination of the normal modes

$$\Phi(0) = c_+\Phi_+ + c_-\Phi_-, \tag{B.6}$$

with c_+ and c_- the linear coefficients of Φ_+ and Φ_-, respectively, so that

$$\Phi(t) = \mathbf{M}\Phi(0) = c_+ e^{\sigma_+ t}\Phi_+ + c_- e^{\sigma_- t}\Phi_-. \tag{B.7}$$

In the stable normal bands σ_+ and σ_- are pure imaginary and

$$\sigma_\pm = B\{2i(\kappa^2 + 1)\beta' \pm i\sqrt{\kappa^8 - 4\kappa^4 + 4\beta'^2}\}. \tag{B.8}$$

In $\langle\phi(t), \phi(t)\rangle$, only coefficients of $\Phi_+^\star\Phi_-$ are functions of time, t. Denoting the complex conjugate with an overbar, we find:

$$\begin{aligned}\langle\phi(t), \phi(t)\rangle = {} & |c_+|^2\Phi_+^\star\Phi_+ + |c_-|^2\Phi_-^\star\Phi_- \\ & + \overline{c_+}c_- e^{\overline{\sigma_+}t} e^{\sigma_- t}\Phi_+^\star\Phi_- \\ & + \overline{c_-}c_+ e^{\overline{\sigma_-}t} e^{\sigma_+ t}\Phi_-^\star\Phi_+,\end{aligned}$$

so that

$$\begin{aligned}\langle\phi(t), \phi(t)\rangle = {} & |c_+|^2\Phi_+^\star\Phi_+ + |c_-|^2\Phi_-^\star\Phi_- \\ & + 2\mathrm{Re}(\overline{c_+}c_- e^{\overline{\sigma_+}t} e^{\sigma_- t}\Phi_+^\star\Phi_-).\end{aligned}$$

$\langle\phi(t), \phi(t)\rangle$ is sinusoidal with time and its period is proportional to:

$$\left|\frac{1}{\overline{\sigma_+} + \sigma_-}\right| = \frac{1}{2B\sqrt{\kappa^8 - 4\kappa^4 + 4\beta'^2}}.$$

This period is thus infinite for wave numbers close to the wave-number cut-offs (κ_{1c}, κ_{2c}). This is why a perturbation with a wave number located in the stable normal band can be very unstable at finite time and be quite comparable to the exponential growth of the unstable normal band.

REFERENCES

Borges, M. D. and Hartmann, D. L. 1992 Barotropic instability and optimal perturbations of observed nonzonal flows. *J. Atmos. Sci.*, **49,** 335–354

Charney, J. G. 1947 The dynamics of long waves in a baroclinic westerly current. *J. Meteorol.*, **4,** 135–162

Davies, H. and Bishop, C. 1994 Eady edge waves and rapid developement. *J. Atmos. Sci.*, **51,** 1930–1946

Eady, E. T. 1949 Long waves and cyclone waves. *Tellus*, **1,** 33–52

Farrell, B. F. 1982 The initial growth of disturbances in a baroclinic flow. *J. Atmos. Sci.*, **39,** 1663–1686

1984 Modal and non-modal baroclinic waves. *J. Atmos. Sci.*, **41,** 668–673

1989 Optimal excitation of baroclinic waves. *J. Atmos. Sci.*, **46,** 1193–1206

Farrell, B. F. and Ioannou, P. J. 1996 Generalized stability theory. Part I: Autonomous operators. *J. Atmos. Sci.*, **53,** 2025–2040

Farrell, B. F. and Moore, A. M. 1992 An adjoint method for obtaining the most rapidly growing perturbation to oceanic flows. *J. Phys. Oceanogr.*, **22,** 338–349

Fischer, C. 1998 Linear amplification and error growth in the 2D Eady problem with uniform potential vorticity. *J. Atmos. Sci.*, **55,** 3363–3380

Held, I. 1985 Pseudomomentum and the orthogonality of modes in shear flow. *J. Atmos. Sci.*, **42,** 2280–2288

Joly, A. 1995 The stability of steady fronts and the adjoint method: Nonmodal frontal waves. *J. Atmos. Sci.*, **52,** 3082–3108

Juckes, M. 1995 Instability of surface and upper-tropospheric shear lines. *J. Atmos. Sci.*, **52,** 3247–3262

Lacarra, J. F. and Talagrand, O. 1988 Short-range evolution of small perturbations in a barotropic model. *Tellus*, **40A,** 81–95

Lorenz, E. N. 1965 A study of the predictability of a 28-variable atmospheric model. *J. Atmos. Sci.*, **17,** 321–333

Moore, A. M. and Farrell, B. F. 1993 Rapid perturbation growth on spatially and temporally varying oceanic flows determined using an adjoint method: Application to the Gulf Stream. *J. Phys. Oceanogr.*, **23,** 1682–1702

O'Brien, E. 1992 Optimal growth rates in the quasi geostrophic initial value problem. *J. Atmos. Sci.*, **49,** 1557–1570

Pedlosky, J. 1987 *Geophysical fluid dynamics*. Springer-Verlag

Phillips, N. A. 1954 Energy transformations and meridional circulations associated with simple baroclinic waves in a two-level, quasi-geostrophic model. *Tellus*, **6,** 273–286

Rotunno, R. and Fantini, M. 1989 Peterssen's 'Type B' cyclogenesis in terms of discrete, neutral Eady modes. *J. Atmos. Sci.*, **46,** 3599–3604

Yoden, S. and Nomura, M. 1993 Finite-time Lyapunov stability analysis and its application to atmospheric predictability. *J. Atmos. Sci.*, **50,** 1531–1543

Warrenfeltz, L. L. and Elsberry, R. L. 1989 Superposition effects in rapid cyclogenesis—linear model studies. *J. Atmos. Sci.*, **46,** 789–802